JOURNAL OF SOLID STATE CHEMISTRY 3, 276–292 (1971)

Mössbauer Study of Phosphides Containing Iron

R. WÄPPLING, L. HÄGGSTRÖM, S. RUNDQVIST, AND E. KARLSSON

Institute of Physics and Institute of Chemistry,
University of Uppsala, Box 530, S-751 21 Uppsala 1, Sweden

Received November 9, 1970

A series of binary and ternary transition metal phosphides containing iron has been investigated by Mössbaue spectroscopy. Most of the compounds studied show complex magnetic behaviour, and interpretations ar proposed for some cases. The crystallographic ordering mechanism in Me_2P-type phosphides is discussed, an it is shown that great care must be taken in assigning the observed components of the Mössbauer spectra t the various crystallographic positions of the iron atoms.

1. Introduction

In the present work the Mössbauer effect has been used to obtain information about the electronic environment and the internal fields acting on iron in several phosphides. It is an extension of earlier work by Rundqvist et al. (*1*, *2*) on the crystal structure of these compounds as determined by X-ray diffraction. Preliminary Mössbauer results for the phosphides of iron have been given earlier (*3*). In this paper we also present results for some ternary transition metal phosphides containing iron.

In the course of these investigations, several papers on identical or closely related compounds have been published. These results are discussed in relation to our own measurements.

2. Crystal Structure Data

Crystallographic data for the binary iron phosphides are summarized in Table I. The structures o all these compounds have been refined from X-ra single-crystal data, and references to this work including descriptions of the structures, are include in the table. Data for the two compounds Co_2P an Ru_2P are also included in Table I. Co_2P and Ru_2 are isostructural and belong to the anti-$PbCl_2$-typ structure.

The present investigation revealed that iron ca substitute for cobalt and ruthenium to a large exte in Co_2P and Ru_2P, respectively, while the anti-$PbCl_2$-type structure is retained. The transitio metal atoms in these phosphides occupy two differ-

TABLE I

CRYSTALLOGRAPHIC DATA FOR THE IRON PHOSPHIDES AND OTHER PHASES USED IN THE INVESTIGATION

Phosphide	Structure type	Space group	Unit cell dimensions (Å)			Ref.
			a	*b*	*c*	
FeP_2	FeS_2 (marcasite), *C*18	*Pnnm*	4.973	5.657	2.723	(*28*)
FeP	MnP, *B*31	*Pnma*	5.191	3.099	5.792	(*29*)
Fe_2P	Fe_2P, *C*22 (revised)	$P\bar{6}2m$	5.865	—	3.456	(*30*)
Fe_3P	Fe_3P, DO_e	$I\bar{4}$	9.107	—	4.460	(*5*)
Co_2P	anti-$PbCl_2$, *C*23	*Pnma*	5.646	3.513	6.608	(*4*)
Ru_2P	anti-$PbCl_2$, *C*23	*Pnma*	5.902	3.859	6.896	(*4*)
NbFeP	anti-$PbCl_2$, *C*23	*Pnma*	6.139	3.585	7.006	(*2*)

ent types of crystallographic position. These were denoted MeI and MeII in (*4*) and the same notation is used in the following. In the ternary $Co_{2-x}Fe_xP$ and $Ru_{2-x}Fe_xP$ phases, the cobalt, ruthenium and iron atoms may populate the MeI and MeII positions in a more or less ordered fashion, depending on the thermal history of the samples.

For the purposes of the present investigation it seemed desirable to obtain a Mössbauer spectrum from a completely ordered anti-$PbCl_2$-type phosphide. Such a spectrum should be a valuable reference for interpreting the spectra from the incompletely ordered $Co_{2-x}Fe_xP$ and $Ru_{2-x}Fe_xP$ phases. A number of ternary anti-$PbCl_2$-type phosphides including ZrFeP and NbFeP were investigated crystallographically in a previous study (*2*). A single-crystal structure analysis of ZrFeP showed that the iron atoms occupy the MeI positions and the zirconium atoms the MeII positions with no measurable disorder. ZrFeP would thus provide a suitable sample for a Mössbauer spectrum of the desired type. Unfortunately, very little ZrFeP was left among the samples from the previous investigation, while a fair amount of pure NbFeP remained. The intensities of the powder diffraction lines for ZrFeP and NbFeP were found to be very closely similar. Intensity calculations assuming various degrees of ordering of the zirconium and iron atoms on the two crystallographic sites in ZrFeP showed that the first few low-angle reflections (which are not very sensitive to moderate changes in the atomic coordinates) were rather sensitive to changes from the ordered distribution. In fact, the changes in the powder line intensities produced by complete disorder or a reversal of the zirconium and iron positions would be so drastic as to be immediately revealed on visual inspection of the powder films. The close similarity between the powder patterns of ZrFeP and NbFeP combined with the fact that zirconium and niobium differ only by one unit in the atomic number is thus considered as conclusive evidence for an essentially ordered distribution of iron atoms on MeI positions and niobium atoms on MeII positions in NbFeP. Accordingly, the NbFeP sample available was used for the Mössbauer work, and its spectrum was interpreted in conformity with the crystallographic analysis given above. Crystallographic data for NbFeP are included in Table I.

The atomic environment of the iron atoms in the phosphides is given in Table II.

TABLE II

ATOMIC ENVIRONMENT OF THE IRON ATOMS IN THE IRON PHOSPHIDES[a]

Phosphide	Central atom	N_{Fe}[b]	d_{Fe}[c]	N_P[d]	d_P[e]
FeP_2	Fe	2	2.72	6	2.26
FeP	Fe	6	2.85	6	2.31
Fe_2P	FeI	8	2.66	4	2.26
	FeII	10	2.84	5	2.46
Fe_3P	FeI	12	2.73	2	2.35
	FeII	10	2.75	4	2.33
	FeIII	10	2.68	3	2.34

[a] Distances shorter than 3.4 Å are taken into account.

[b] N_{Fe} = Number of iron neighbours.

[c] d_{Fe} = Average distance (Å) between the central atom and its iron neighbours.

[d] N_P = Number of phosphorus neighbours.

[e] d_P = Average distance (Å) between the central atom and its phosphorus neighbours.

3. Sample Preparation

Iron phosphide samples were prepared from spectroscopically standardized iron rods (Johnson, Matthey & Co., Ltd., London) and red phosphorus (purity higher than 99%) using the same technique as described in (*5*). On analysis, phosphides synthesized in this way have given totals for iron and phosphorus between 99.94 and 100.02%. Judging from strongly exposed X-ray powder diffraction films, the samples used in the Mössbauer measurements contained no detectable amounts of neighbouring phases in the Fe–P system.

In the case of FeNbP we used a previously prepared sample (*2*), as was discussed in Section 2.

The $Co_{2-x}Fe_xP$ and $Ru_{2-x}Fe_xP$ samples were prepared by heating mixtures of the component elements (metals with purity higher than 99.8% and phosphorus with purity higher than 99%) in evacuated and sealed silica tubes. The annealing conditions have a strong influence on the degree of ordering of the metal atoms on the two types of crystallographic positions in the structure and details of the various heat treatments are, therefore, given below in connection with the results of the Mössbauer measurements. The purity and homogeneity of each sample was checked by careful inspection of strongly exposed X-ray powder diffraction films. X-ray diffraction patterns were recorded in Guinier–Hägg type focussing cameras using strictly monochromatic Cr K_{α_1} radiation. Silicon ($a = 5.43054$ Å) was used as internal calibration standard.

4. Experimental Details

The samples were crushed to a fine powder and spread on self-adhesive tape. In this way suitable

Mössbauer absorbers were obtained with a thickness of 20–30 mg/cm^2. The source was ^{57}Co in a palladium matrix giving a single emission line, and spectra were recorded using a constant acceleration spectrometer (*6*). The obtained spectra were decomposed using a least-squares computer fit, and the quoted errors are those given by the computer. Measurements were made at room temperature and at liquid nitrogen temperature. In some cases also intermediate temperatures were used. In most of the measurements the source was kept at room temperature giving rise to a second-order Doppler shift in the low-temperature measurements. In the measurements on Fe_3P an external magnetic field, parallel to the observation direction, was also applied on the absorber. The spectrometer was calibrated by recording the spectrum of iron metal.

5. Experimental Results

For convenience, we give the results for the different compounds under separate headings.

5.1. FeP_2

The room-temperature spectrum of FeP_2 is shown in Fig. 1, and it is within experimental errors identical with the spectrum obtained at 80°K. The experimental values are given in Table III and agree reasonably well with the values reported by Gérard (*7*).

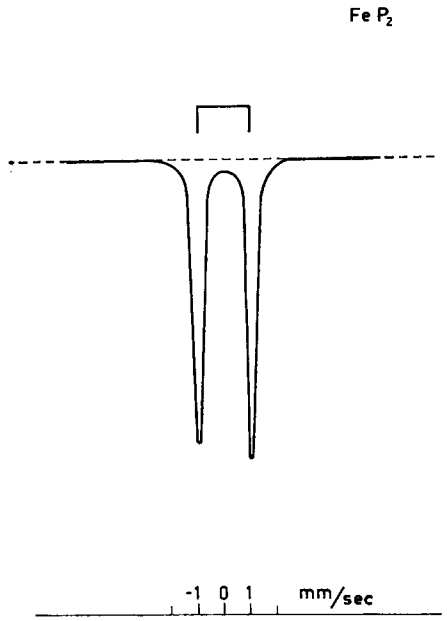

FIG. 1. Mössbauer spectrum for FeP_2 at 295°K.

TABLE III

ISOMER SHIFTS AND QUADRUPOLE SPLITTINGS IN LÖLLINGITE

Compound	T (°K)	Isomer shift[a] (mm/sec)	Quadrupole splitting (mm/sec)	Ref.
FeP_2	295	0.09 ± 0.03	2.08 ± 0.02	Present work
	80	0.07 ± 0.02	2.06 ± 0.02	
$FeAs_2$	295	0.310 ± 0.007	1.68 ± 0.04 1.71 ± 0.04	(*9*)
$FeSb_2$	295	0.451 ± 0.005	1.281 ± 0.016	(*10*)
	81	0.565 ± 0.005	1.585 ± 0.019	

[a] Isomer shifts versus natural iron, Tables III and IV.

From the crystal-chemical point of view, FeP_2 is classified as a member of the löllingite branch of the marcasite-type structure (*8*). Other members of this branch are $FeAs_2$ and $FeSb_2$. Both of these compounds have been investigated earlier using the Mössbauer effect (*9*, *10*) and the results are given in Table III. The isomer shift for FeP_2 is [according to the model given by Danon (*11*)] consistent with a pure d^4-electron configuration for iron, while the increase in isomer shift for $FeAs_2$ and $FeSb_2$ can be explained by covalency effects increasing the effective number of d electrons on the iron ions. The observed decrease in quadrupole splitting in going from FeP_2 to $FeSb_2$ can be correlated with the interatomic distances in the compounds and the filling of $3d$ orbitals through the covalency effect mentioned above.

5.2. FeP

Several investigations of the magnetic properties of FeP have been performed giving contradictory results. Shu Shiba (*12*) first reported FeP to be paramagnetic with a typical Curie-Weiss behaviour in the temperature region 290–900°K. Cadeville (*13*) in a later study reported that FeP was ferromagnetic with a Curie temperature of 215°K. Above this temperature, FeP followed the Curie–Weiss law but with constants differing considerably from those given in (*12*). Stein and Walmsley (*14*) observed essentially temperature-independent paramagnetic behaviour as determined by their susceptibility measurements. In their NMR measurements they observed, below 120°K, an unresolved structure which they attributed to magnetic impurities since the resonance signal from ^{31}P is insensitive to electric quadrupole interactions. Roger and Fruchart

(*15*) and Bonnerot et al. (*16*) have observed temperature-independent paramagnetic properties in their susceptibility, resistivity, and specific heat measurements.

The main reason for these conflicting results lies presumably in the difficulty to prepare a well-defined homogenous phase of FeP. In a recent study, Bellavance et al. (*17*) have prepared single crystals of FeP using two different methods; namely, electrolytical and chemical transport methods. These authors have also performed physical measurements on the samples. The resistivity shows a typical metallic temperature dependence. There is, however, an inflection point at about 120°K. The susceptibility has a constant value of about 3.7×10^{-6} emu/g between 140°K and room temperature. Below 140°K, the susceptibility decreases to about 3.1×10^{-6} emu/g at 65°K and then starts to increase.

Gérard (*7*) performed Mössbauer measurements at 300 and 120°K and obtained, within experimental error, identical results for the two temperatures. He observed a quadrupole splitting of 0.7 mm/sec and an isomer shift of 0.5 mm/sec (with respect to stainless steel). Bailey and Duncan (*18*) later reported a well-resolved doublet at 293°K in agreement with Gérard's result. At liquid air temperature (90°K) they obtained a broad single asymetric absorption line which they interpreted as due to two nonequivalent iron sites in the lattice. Senateur et al. (*19*) in a very recent paper reproduced the earlier room-temperature results. At temperatures below 126°K, they report a broadening of the two peaks persisting all the way down to 1.5°K. This broadening gives, below 90°K, a single asymetric absorption line. From these results they conclude that FeP is antiferromagnetic with a Néel temperature of 126°K.

The last mentioned results are in agreement with ours (see Fig. 2), which also show a broadening at 80°K. However, the doublet is well resolved in our measurement. By assigning the broadening to a magnetic interaction, it is possible to give an upper value of the magnetic field equal to 6 kG. A magnetic interaction would also give an asymmetry as indicated in Fig. 2(b), since one of the components of the doublet involves the $m = \pm\frac{3}{2}$ to $m = \pm\frac{1}{2}$ transition which is more sensitive to magnetic fields and, therefore, will show a larger broadening than the other component of the doublet which involves only magnetic nuclear quantum numbers equal to $\pm\frac{1}{2}$.

The value of the magnetic field corresponds to a magnetic moment of about 0.05 μB. It would be interesting to compare this value with the neutron measurements by Felcher et al. [mentioned in the paper by Bellavance et al. (*17*)]. The neutron diffraction work reveals that FeP is an antiferromagnetic spiral at 77°K but has no observable spin ordering at room temperature (*17*). Complete results have, however, not yet been published.

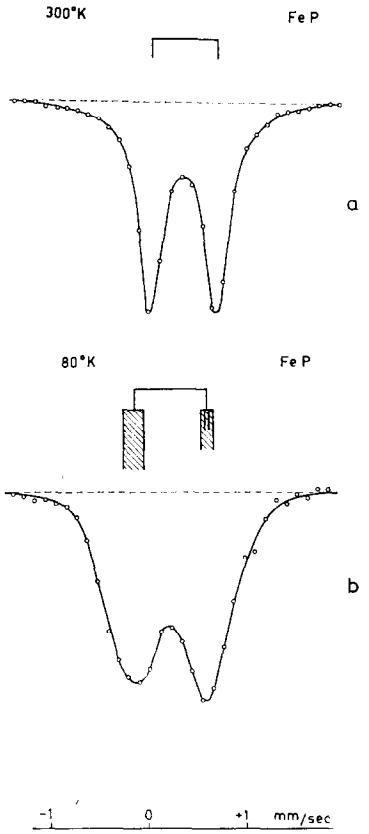

FIG. 2. Mössbauer spectrum for FeP (a) at room temperature and (b) at 80°K.

The experimental data for FeP can be most simply interpreted in the following way. From room temperature to about 130°K FeP is a Pauli paramagnet. Below this temperature an antiferromagnetic spiral (or possibly in view of the similarity with MnP, a double spiral) is developed, and at low temperatures a slight ferromagnetic moment forms through spin canting, giving the increase in susceptibility found by several investigators. The origin of the magnetic ordering is not very clear, but it seems tempting to suggest that itinerant electrons are responsible, through a spin-density wave model. A measurement of the specific heat on passing the Néel point should constitute a valuable test of the magnetic-ordering mechanism since in the proposed model a very slight discontinuity is expected [cf. chromium metal (*20*)] as compared to the marked discontinuity in a localized spin model. Further Mössbauer measurements at low temperatures are in progress.

5.3. Fe_2P

The magnetic properties of Fe_2P have been studied by Cadeville (*13*). From susceptibility measurements, she concluded that stoichiometric Fe_2P is a ferromagnet with a Curie temperature of 266°K and a saturation moment of 2.75 μB per formula unit. Mössbauer data on this phosphide have been reported by several authors (*7, 18, 21, 22*). These authors have all resolved the room-temperature spectrum into three lines. By using low velocities in recording the spectrum it is, however, possible to get enough detailed information to resolve the spectrum into four lines [Fig. 3(a)]. There are two different crystallographic positions for iron in the hexagonal Fe_2P structure (see Table II), and through electric quadrupole interactions, two lines are obtained for each iron site in the nonmagnetic state. As is evident from Fig. 3(a), the intensities of two of the lines are different from the intensities of the other two lines. There might be several reasons for this to occur:

(I) A preferred orientation of the powder in the absorber used.
(II) Vacancies on one of the crystallographic positions (nonstoichiometry).
(III) Different recoil-free fractions (Debye temperatures) for the two positions.

If there is a preferred orientation, one would obtain different intensities by varying the angle between the absorber and the γ-ray direction. Such a check was performed by turning the absorber 45° and recording a spectrum. No change was obtained as compared to the spectrum in Fig. 3(a). This rules out possibility (I). The choice between the two other possibilities can be made by looking at Fig. 3(b), which shows

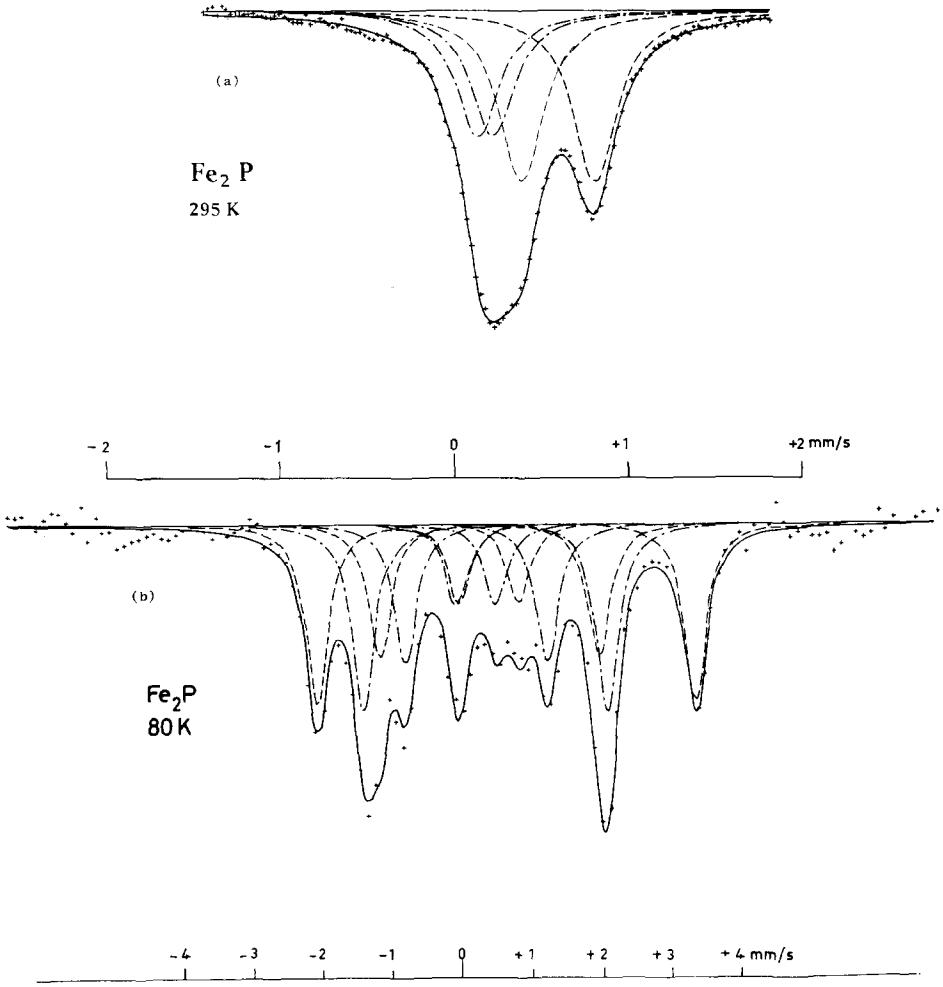

FIG. 3. Mössbauer spectrum for Fe_2P (a) at room temperature and (b) at 80°K.

TABLE IV

SUMMARY OF EXPERIMENTAL RESULTS ON ISOMER SHIFTS, QUADRUPOLE SPLITTINGS, AND MAGNETIC SPLITTINGS FOR IRON-CONTAINING Me_2P-PHOSPHIDES

		MeI				MeII			
Temperature (°K)	Absorber	Magnetic field (kG)	Isomer shift (mm/sec)	Electric splitting (mm/sec)	Intensity	Magnetic field (kG)	Isomer shift (mm/sec)	Electric splitting (mm/sec)	Intensity
295	FeNiP	—	0.609 ± 0.001	0.430 ± 0.002	1.0	—	0.187 ± 0.001	0.095 ± 0.003	0.857 ± 0.008
295	Fe_2P	—	0.600 ± 0.001	0.427 ± 0.001	1.0	—	0.182 ± 0.001	0.088 ± 0.003	0.739 ± 0.005
295	FeNbP	—	0.269 ± 0.001	0.338 ± 0.002	1.0	—	—	—	—
295	FeRuP (annealed 1 week)	—	0.385 ± 0.005	0.396 ± 0.008	1.0	—	0.768 ± 0.000	0.821 ± 0.015	0.484 ± 0.024
295	FeRuP (annealed 3 weeks)	—	0.273 ± 0.005	0.346 ± 0.004	1.0	—	0.637 ± 0.005	0.903 ± 0.012	0.290 ± 0.008
295	FeCoP	29.9 ± 0.3	0.278 ± 0.004	1.166 ± 0.024	1.0	146.2 ± 0.1	0.584 ± 0.001	−0.766 ± 0.004	4.41 ± 0.05
80	FeNiP	160.9 ± 0.2	0.660 ± 0.002	0.224 ± 0.004	1.0	101.2 ± 0.2	0.376 ± 0.002	0.122 ± 0.003	1.066 ± 0.016
80	Fe_2P	169.3 ± 0.5	0.515 ± 0.005	0.248 ± 0.010	1.0	109.1 ± 0.5	0.271 ± 0.005	0.124 ± 0.009	1.045 ± 0.055
80	FeNbP	—	0.373 ± 0.001	0.358 ± 0.002	1.0	—	—	—	—
80	$Fe_{1.8}Co_{0.2}P$	70.0 ± 0.5	0.306 ± 0.006	0.036 ± 0.009	1.0	147.7 ± 0.2	0.703 ± 0.004	0.067 ± 0.007	1.412 ± 0.028
100	FeCoP	47.0 ± 0.6	0.380 ± 0.005	1.169 ± 0.005	1.0	187.4 ± 0.1	0.690 ± 0.001	−0.861 ± 0.005	4.81 ± 0.05

the spectrum recorded at 80°K. Here the intensities of the two sets are within experimental errors equal (see also Table IV). This rules out the second possibility, and we conclude that the observed effect is due to different Debye temperatures for the two crystallographic positions. Since it is possible from X-ray diffraction measurements to get information on the lattice vibrations through the "temperature factors", the observed intensity difference can serve as a guide in assigning the observed sets of lines to crystallographic positions. This will be discussed further in Section 6.

The results are summarized in Table IV. The room-temperature values are in reasonable agreement with those reported by Bailey and Duncan (*18*) and Fruchart et al. (*22*). Low-temperature data for Fe_2P have been given in (*7*), (*18*), and (*21*). The results of Bailey and Duncan show a marked discrepancy from the other authors' values and from the present ones. The origin of this discrepancy is evidently due to too small a velocity range in recording the spectrum leading to the neglect of the absorption line at +3.37 mm/sec.

5.4. FeNiP

The system, $Fe_{2-x}Ni_xP$, forms a complete solid solution in the hexagonal phase (*22*), and here we chose to study only the composition of FeNiP. Fruchart et al. report for this compound a Curie temperature of about 95°K and a relatively high degree of crystallographic ordering (about 75% of the iron atoms on one of the metal positions) (*22*).

Our sample of FeNiP shows almost no crystallographic ordering [e.g., Fig. 4(a) is almost identical

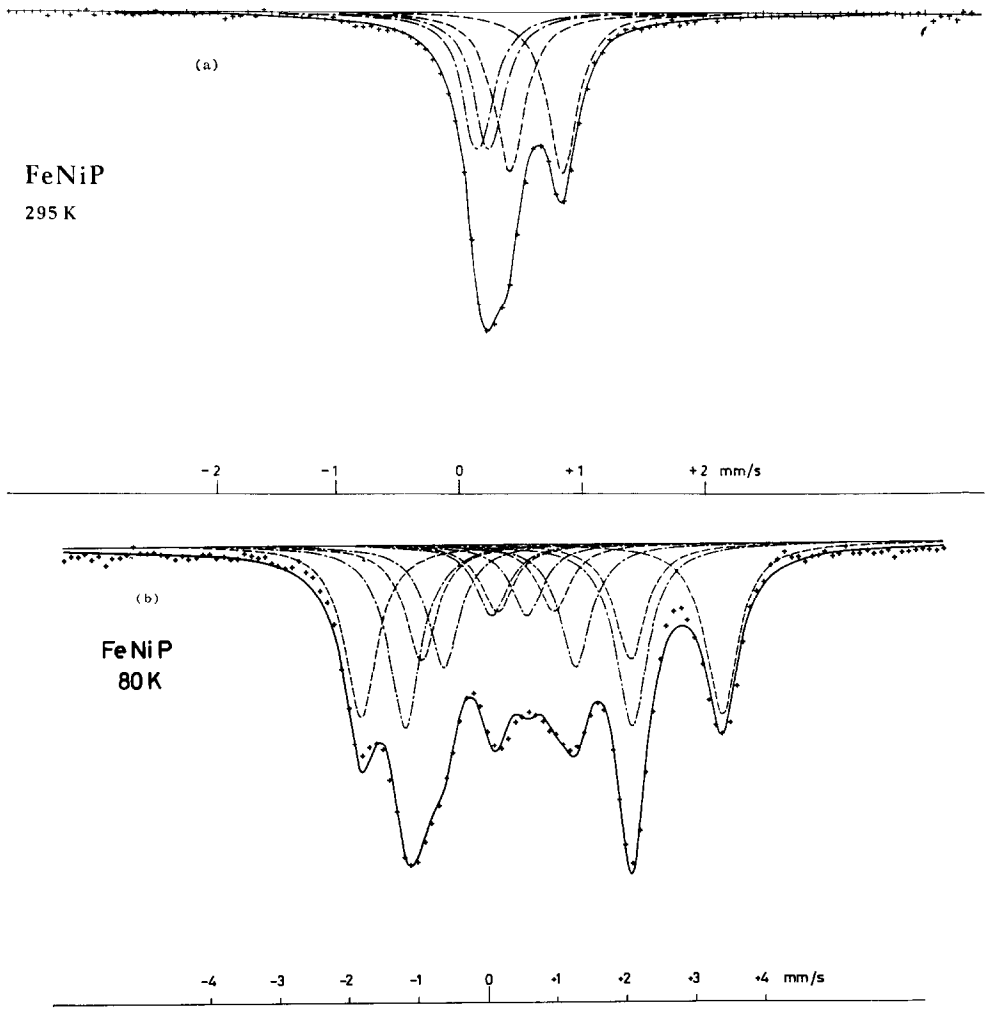

FIG. 4. Mössbauer spectrum for FeNiP (a) at room temperature and (b) at 80°K.

to Fig. 3(a)] which indicates that the ordering parameters are very sensitive to the thermal treatment of the samples. Fruchart et al. synthesized their samples by solid-phase diffusion at temperatures between 850 and 950°C, while our sample was heated at 1000°C for 4 days and subsequently slowly cooled.

Our sample also gives a Curie temperature of about 190°K, i.e., about twice the value reported in (*22*). However, it is evident from the Curie temperature versus the composition curve given in (*22*) that even small changes in composition produce large changes in the Curie temperature. It is also possible that the crystallographic ordering might affect the magnetic properties. The Curie temperature was measured by recording Mössbauer spectra at various temperatures and can, therefore, not be due to impurity phases present.

In FeNiP we observe the same intensity difference as in Fe_2P, indicating different Debye temperatures for the two crystallographic positions [Fig. 4(a)]. The low-temperature spectra of Fe_2P and FeNiP are also very similar, as can be seen on comparing Figs. 3(b) and 4(b). The results are included in Table IV, and it is seen that the hyperfine fields in FeNiP are somewhat lower than the values for Fe_2P. This reflects the difference in Curie temperatures, Fe_2P being closer to saturation at 80°K. The isomer shifts are larger in FeNiP indicating an increase in the effective number of *d* electrons on the iron ions.

5.5. $Co_{2-x}Fe_xP$

This system has also been studied by Fruchart et al. (*22*), and since their experimental results largely agree with ours, we only present a short summary

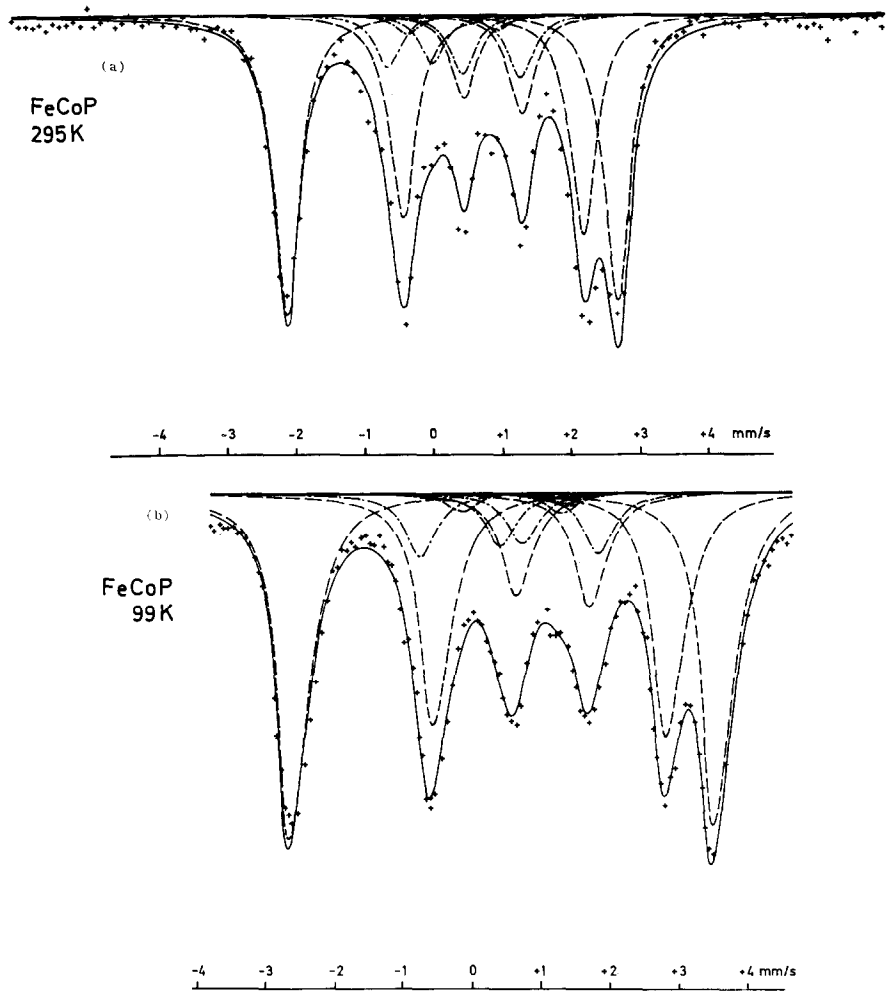

FIG. 5. Mössbauer spectrum for FeCoP (a) at room temperature and (b) at 100°K. These two spectra consist of 16 lines; however, four lines are very weak.

of our measurements. We have recorded Mössbauer spectra for compositions corresponding to $x = 0.5$, 1.0, 1.5, and 1.8, and the spectra of FeCoP and the low-temperature spectrum of $Fe_{1.8}Co_{0.2}P$ are shown in Figs. 5 and 6, respectively. The results for FeCoP are given in Table IV. The data have been analysed by diagonalization of the full Hamiltonian (*23*), and making a least-squares fit to the data. The dependence of the asymmetry parameter η, and the azimuthal angle ϕ on the spectra is very weak. For the room-temperature spectrum, we, therefore, fixed η and ϕ to 0.0 in the fitting, yielding the values in Table IV. The angle θ, which is the angle between the magnetic field vector **B** and the largest component (V_{ZZ}) of the diagonalized electric field gradient tensor, which was including as a variable in the fitting, turns out to be $(36 \pm 1)°$ for MeI site and $(16.8 \pm 0.1)°$ for the MeII site.

The spectrum recorded at 100°K was more sensitive for various η and ϕ values on the MeI site, while for the MeII site we get weak dependence on these variables. Our fitting gives $\eta = 1.0 \pm 0.2$, $\phi = (126.1 \pm 3.1)°$, and $\theta = (126 \pm 1)°$ for MeI, and $\theta = (19.7 \pm 0.2)°$ for MeII. The other variables are presented in Table IV. The θ values for MeII are in good agreement with the qualitative result given by Fruchart et al. (*22*).

A description of this least-square fit program, which is a development of the program by Agresti et al. (*31*), will be published later. The program is written in FORTRAN IV, and one can make the fitting procedure with all variables occurring in the full Hamiltonian.

At the composition, $Fe_{1.8}Co_{0.2}P$, we find surprisingly small quadrupole splittings at low temperatures. At room temperature, we only obtain a broad absorption indicating that the Curie temperature is only slightly above 300°K. Our sample had the anti-$PbCl_2$-type structure, whereas from (*22*) we would expect the hexagonal Fe_2P-type structure. This observation puts further emphasis on the critical influence of the thermal history of the samples on the properties observed.

5.6. FeNbP

As is evident from Fig. 7, FeNbP is crystallographically ordered, in agreement with the X-ray diffraction results discussed in Section 2. Furthermore, there is no magnetic transition above 80°K. This compound was investigated in order to get further information on the electric quadrupole interaction for iron in the orthorhombic structure in a situation where it is clear which of the two crystallographic positions that is populated by the iron atoms. The X-ray diffraction data quite conclusively show that iron occupies the MeI position, and niobium the MeII position (see Section 2). We thus obtain an isomer shift of 0.27 mm/sec and a quadrupole splitting of 0.34 mm/sec (Table IV) for iron on the MeI position. This is in quite good agreement with the results for FeRuP which are discussed below.

5.7. $Ru_{2-x}Fe_xP$

Since iron and ruthenium both have eight electrons outside their noble gas cores, it is interesting to investigate the Mössbauer spectra of solid solutions containing the two transition metals. We have chosen to study the $Ru_{2-x}Fe_xP$ system in order to

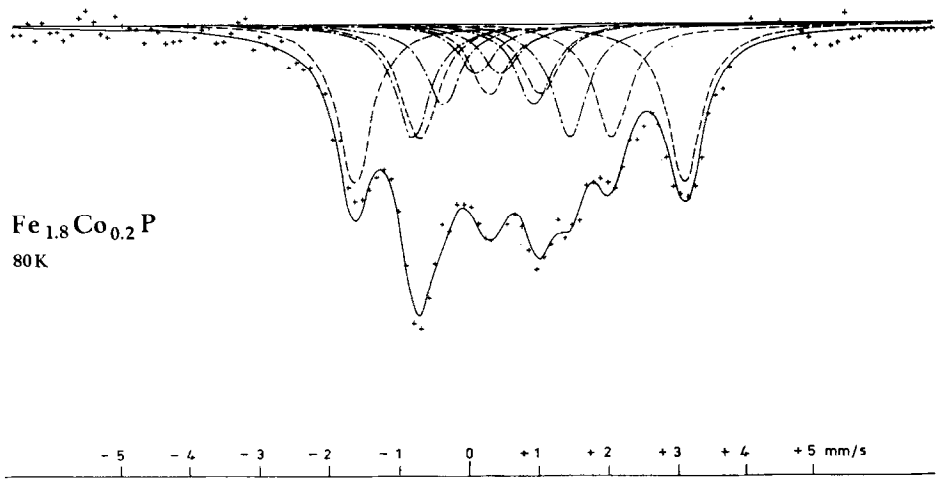

FIG. 6. Mössbauer spectrum for $Fe_{1.8}Co_{0.2}P$ at 80°K.

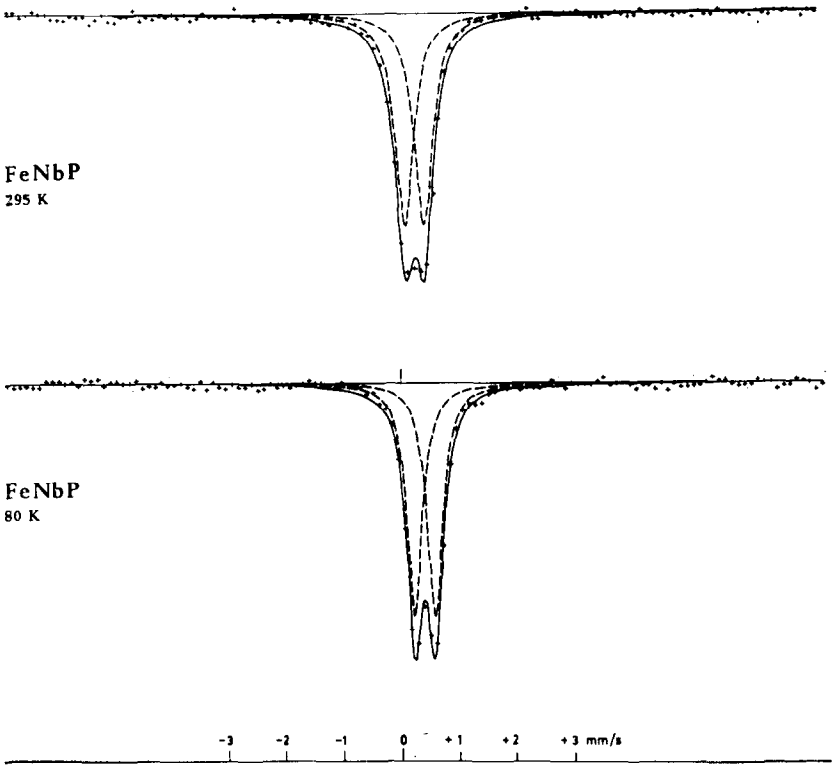

FIG. 7. Mössbauer spectrum for the ordered FeNbP (a) at room temperature and (b) at 80°K.

see whether any crystallographic ordering exists in the system and how the magnetic properties change on substituting iron for ruthenium. The magnetic properties of this system will be reported elsewhere in connection with angular correlation measurements on ruthenium in FeRuP.

Single-phase samples with $x = 0.5$, 1.0, and 1.5 were investigated, and room-temperature spectra are shown in Fig. 8. It is evident that even in strong excess of ruthenium the iron atoms populate both MeI and MeII-type positions, since two different iron signals are obtained. (This is also in agreement with the X-ray diffraction data.)

The ordering process in the FeRuP sample was investigated as follows. The sample was annealed at 1050°C for 1 week, and the powder diffraction pattern and the Mössbauer spectrum were recorded. The annealing was then prolonged for another 2 weeks at 1050°C, after which the diffraction pattern and the Mössbauer spectrum were again recorded. The analysis of the Mössbauer spectra showed that about 30% of the iron atoms occupied one type of crystallographic position and the remaining 70% the other type of position. The values for the quadrupole splitting and isomer shift for the latter type of iron atoms corresponded closely to the values for the MeI-type iron atoms in NbFeP. Intensity calculations for the powder diffraction lines of FeRuP, assuming different distributions of iron and ruthenium on the MeI and MeII positions, were compared with the diffraction patterns recorded. Visual inspection of the film from the 1-week sample indicated a rather even distribution of iron on the two sites with a tendency towards preferential occupation of the MeI sites by the iron atoms. When this film was compared with the diffraction film taken after prolonged annealing, significant changes in line intensities were observed. These changes were, without exception, consistent with an increased population by iron atoms of the MeI-type sites. The intensity distribution calculated on the assumption of a 75% iron occupation of site MeI and 25% of MeII was in good qualitative agreement with the visually observed intensities of the reflections from the sample annealed for three weeks.

Both Mössbauer and diffraction data thus consistently indicate that the iron atoms predominantly populate the MeI-type crystallographic sites in properly annealed RuFeP samples.

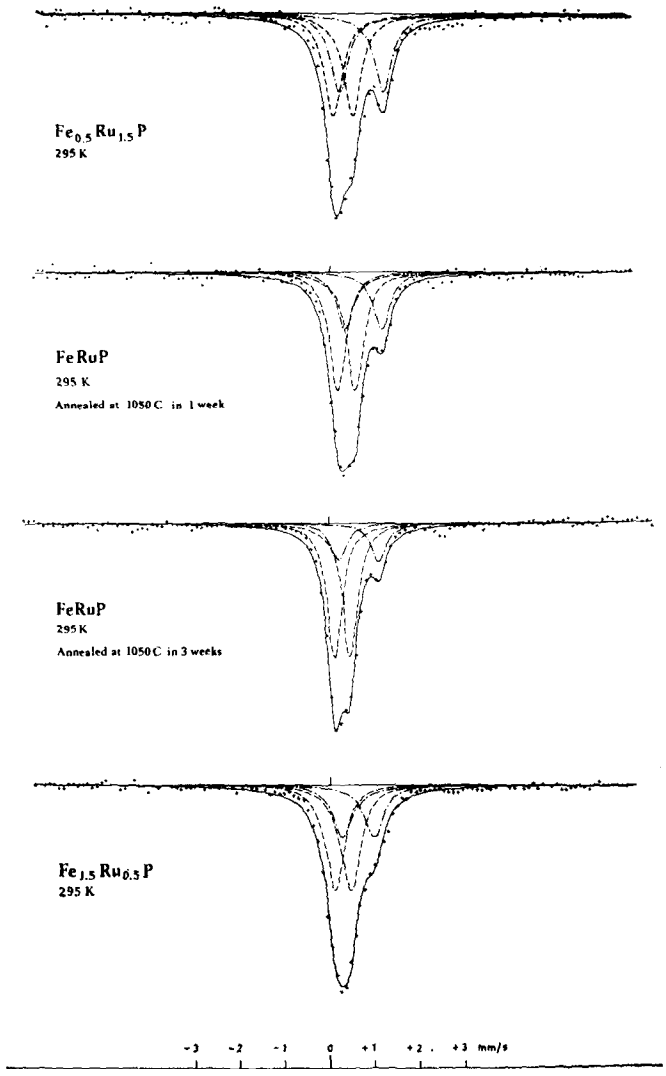

Fig. 8. Mössbauer spectrum for $Ru_{2-x}Fe_xP$ at room temperature.

5.8. $Fe_3P_{1-x}B_x$

Due to the difficulty in interpreting the spectrum of Fe_3P (*3*) it was decided to investigate the effect on the Mössbauer spectrum when boron was introduced, replacing phosphorus.

The line $Fe_3P_{1-x}B_x$ ($0 \leqslant x \leqslant 1$) in the isothermal section at 1000°C of the Fe–P–B equilibrium diagram has been previously studied crystallographically by Rundqvist (*5*). The samples used in the present study were selected from those investigated in (*5*). The sample with composition $Fe_{2.88}P_{0.05}B_{0.95}$ should contain some Fe_2B, whereas the other samples represented single phases. Since the Mössbauer spectrum of Fe_2B is known (*24*), the presence of this phase should not be very disturbing.

Cadeville reported that Fe_3P is a ferromagnet with a Curie temperature of 716°K and an average moment per iron atom of 1.86 μB (*13*). In a later study of $Fe_3P_{1-x}B_x$ samples by thermomagnetic methods, Fruchart et al. (*25*) obtained the following values for Fe_3P: Curie temperature, 686°K, average magnetic moment, 1.91 μB per iron atom. Mössbauer data for Fe_3P have been given by Bailey and Duncan (*18*). They have resolved their spectrum into three sets of lines, one for each iron position, and obtained values for the hyperfine fields, isomer shifts, and quadrupole splittings. The published spectrum also revealed a large spread in the measured points due probably to low counting statistics.

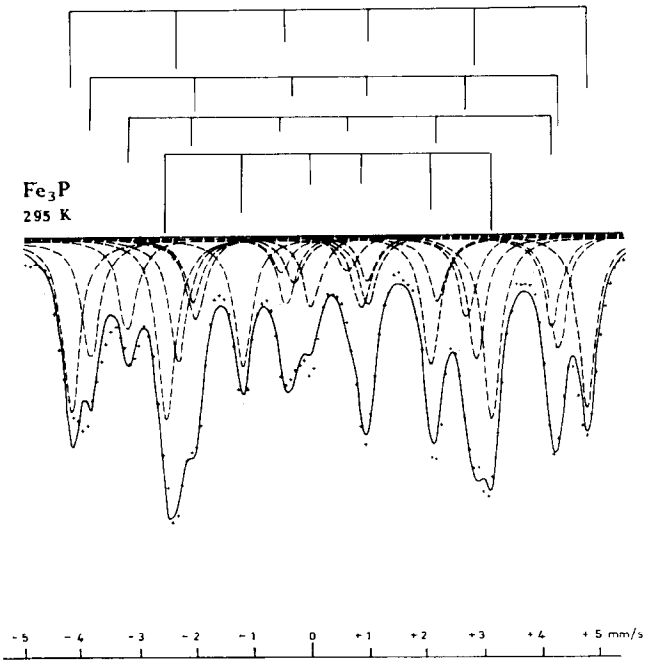

FIG. 9. Mössbauer spectrum for Fe_3P at room temperature.

The spectrum obtained for Fe_3P in the present investigation is shown in Fig. 9. It turns out that it is impossible to resolve this spectrum into only three sets of lines. In order to reduce the number of absorption lines, a separate measurement was made in an external magnetic field of 33 kG, parallel to the direction of the γ rays. The resulting spectrum is shown in Fig. 10. The experimental geometry was, in this measurement, such that it was very difficult to obtain a high statistical accuracy. Nevertheless, the data obtained were sufficient for drawing the following conclusions. In the high external field the sample should be completely polarized, and all the absorption lines corresponding to transitions with no change in nuclear magnetic quantum number should vanish, since the γ-ray transition is of dipole character. This effect was observed in our experiment. Furthermore, the effective magnetic field at the nucleus will change in magnitude, due to the addition of the external field. The observed effect corresponds to a decrease in overall splitting, indicating that the hyperfine field is negative. The overall shape of the spectrum is preserved, indicating an essentially parallel spin orientation in Fe_3P. There are, however, indications (especially marked in the broad absorption line at -3.5 mm/sec) that the finer

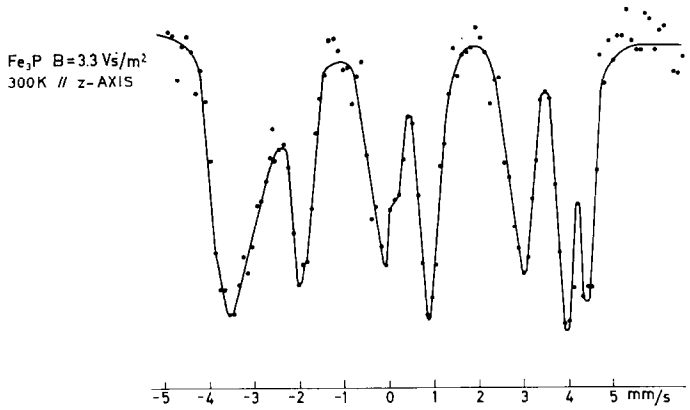

FIG. 10. Mössbauer spectrum for Fe_3P in a magnetic field of 3.3 Vsec/m^2 parallel to the z axis at room temperature.

details of the spectrum might be changed. By comparison with Fig. 9, it appears that the lines corresponding to the third largest hyperfine field do not shrink as much as the other three sets. This could be taken as evidence that the spin orientation for this component is not parallel to the others.

The spin structure of Fe_3P is being investigated by Wilkinson (*26*) by neutron diffraction, and the preliminary experimental results suggest a more complicated spin arrangement than in a simple ferromagnet. In view of the present Mössbauer results, we propose that Fe_3P has a spin structure with a larger number of nonequivalent "magnetic" iron positions (that is, positions in the magnetic unit cell) than "chemical" positions. At least four magnetically nonequivalent types of iron atoms can be distinguished in the Mössbauer spectrum.

The results for the boron substituted samples are shown in Figs. 11–13 and are summarized in Table V. It is seen that for the most phosphorus-rich ones (Fig. 11), it is necessary to assume at least four different sets of lines, whereas for the more boron-rich samples [which also correspond to a structure different from Fe_3P as described in (*5*)] it is possible to get a reasonably good fit with only three sets of lines (Figs. 12 and 13). The intensities of the resolved lines are, however, such that a very complicated magnetic structure must be invoked to explain the results. No evidence was found for a relevant effect of the Fe_2B impurity in the spectrum in Fig. 13.

6. Discussion

It is evident from the present investigation that the iron-containing phosphides of transition metals exhibit a rather complicated magnetic behaviour. FeP_2, showing no magnetic ordering in the temperature range studied, is the simplest case and it is sufficient, at the moment, to say that FeP_2 fits rather nicely into the series of other isostructural iron compounds. But already the next binary phosphide FeP, is complicated from the magnetic point of view. The magnetic moment of the iron atoms is unusually small. Although, in the present experiment we had not reached saturation, it seems that the saturation magnetic moment would certainly be less than 0.1 μB.

As concerns the Me_2P-phosphides, it is of particular interest to assign the observed sets of absorption lines to the appropriate crystallographic positions. In the anti-$PbCl_2$-type structures, this is indeed possible as described in Subsections 5.6 and 5.7. The more intense lines in FeRuP are due to iron on the MeI position. The two weaker lines then reveal that on the MeII position the iron nuclei experience a larger electric field gradient (EFG) giving a larger quadrupole splitting. In fact the splitting is so large (0.90 mm/sec) that there must be a contribution to the EFG from the atomic electrons for iron on the MeII position, presumably in a d^6 configuration. This is also in accordance with the value of the isomer shift (0.64 mm/sec).

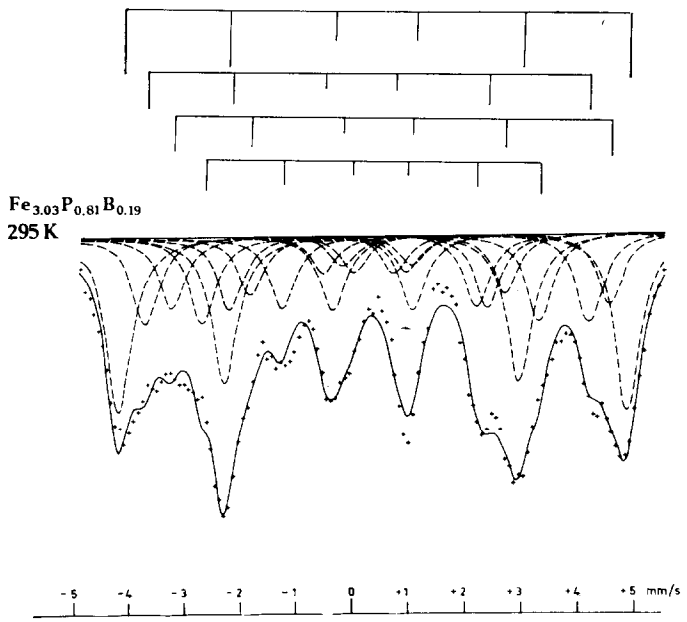

FIG. 11. Mössbauer spectrum for $Fe_{3.03}P_{0.81}B_{0.19}$ at room temperature.

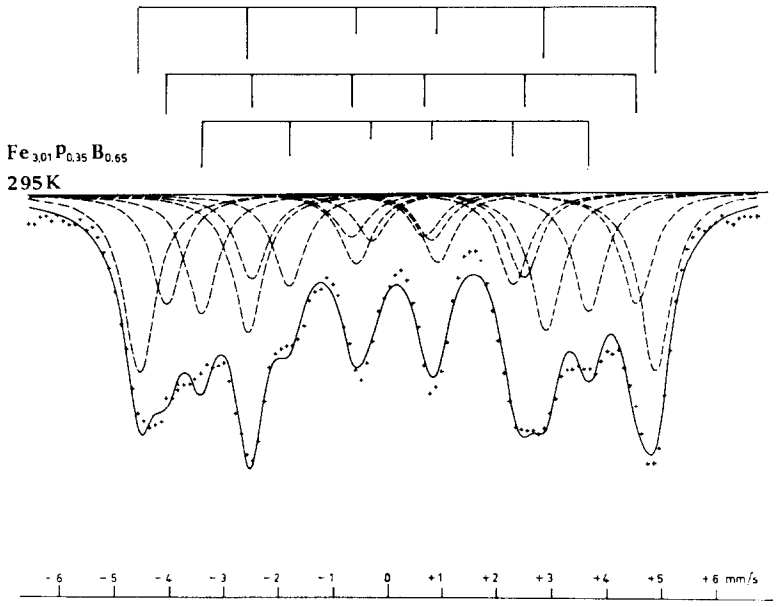

FIG. 12. Mössbauer spectrum for $Fe_{3.01}P_{0.35}B_{0.65}$ at room temperature.

Turning to $Co_{2-x}Fe_xP$, it should be possible to extrapolate the above-mentioned results to this series of solid solutions. If we look at the results for FeCoP we find also here one value for the isomer shift consistent with a d^6 configuration (0.57 mm/sec) and one value consistent with a d^5 configuration. The associated quadrupole splittings are 0.43 and −0.57 mm/sec, respectively. The value for a pure d^5 configuration represents the lattice contribution to the EFG and should have a larger value in FeCoP than in FeRuP, due to the shorter interatomic distances in FeCoP.

This is also borne out by the experiment and the reduced quadrupole splitting for the d^6 configuration can be explained accordingly since the calculations by Ingalls (*27*) shows that the electron and

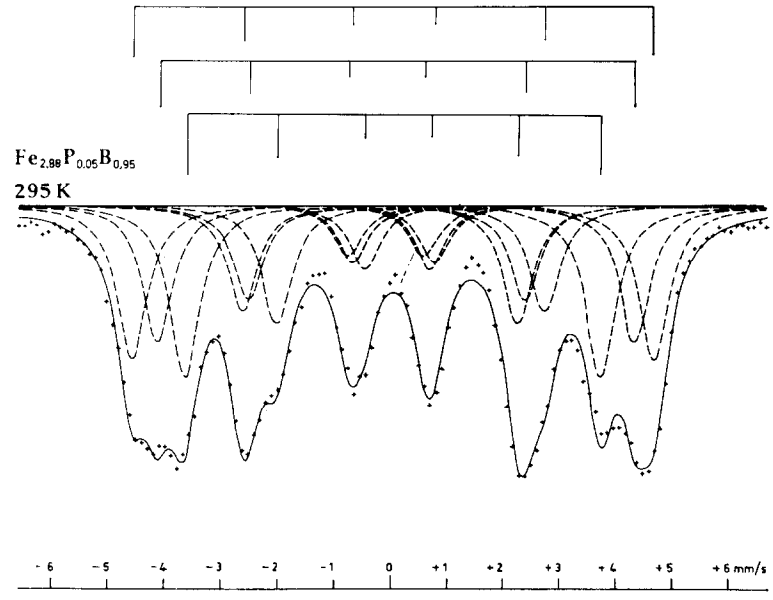

FIG. 13. Mössbauer spectrum for $Fe_{2.88}P_{0.05}B_{0.95}$ at room temperature.

TABLE V

SUMMARY OF EXPERIMENTAL RESULTS ON ISOMER SHIFTS, QUADRUPOLE SPLITTINGS AND MAGNETIC SPLITTINGS FOR THE SERIES $Fe_3P_{1-x}B_x$

	FeI				FeII			
Absorber	B	δ[a]	ΔE_Q[b]	I[c]	B[d]	δ	ΔE_Q	I
Fe_3P	278.7 ± 0.1	0.287 ± 0.001	0.034 ± 0.001	30.8 ± 1.0	251.7 ± 0.1	0.280 ± 0.001	−0.122 ± 0.002	20.6 ± 1.0
$Fe_{3.03}P_{0.81}B_{0.19}$	281.6 ± 0.1	0.257 ± 0.001	0.019 ± 0.001	41.7 ± 0.5	246.1 ± 0.2	0.078 ± 0.002	0.149 ± 0.003	20.9 ± 0.5
$Fe_{3.01}P_{0.35}B_{0.65}$	293.1 ± 0.2	0.164 ± 0.001	0.006 ± 0.003	43.7 ± 1.0	267.1 ± 0.3	0.119 ± 0.002	0.245 ± 0.005	27.1 ± 1.5
$Fe_{2.88}P_{0.05}B_{0.95}$	288.6 ± 0.2	0.094 ± 0.001	−0.002 ± 0.002	33.3 ± 1.0	263.8 ± 0.2	0.057 ± 0.002	0.183 ± 0.003	29.5 ± 1.4
	FeIII				FeIV			
Absorber	B	δ	ΔE_Q	I	B	δ	ΔE_Q	I
Fe_3P	175.6 ± 0.1	0.367 ± 0.001	−0.136 ± 0.001	32.5 ± 1.0	228.4 ± 0.1	0.271 ± 0.002	0.435 ± 0.003	16.1 ± 1.0
$Fe_{3.03}P_{0.81}B_{0.19}$	186.7 ± 0.2	0.294 ± 0.001	−0.160 ± 0.003	20.6 ± 0.5	242.4 ± 0.2	0.448 ± 0.003	0.235 ± 0.003	16.8 ± 0.7
$Fe_{3.01}P_{0.35}B_{0.65}$	220.6 ± 0.2	0.185 ± 0.002	−0.118 ± 0.004	29.2 ± 1.2				
$Fe_{2.88}P_{0.05}B_{0.95}$	229.7 ± 0.1	0.123 ± 0.001	−0.083 ± 0.003	37.2 ± 1.1				

[a] δ represents isomer shift in mm/sec versus natural iron.
[b] ΔE_Q represents electric splitting in mm/sec.
[c] I represents relative intensity.
[d] B represents magnetic field in kG.

lattice contribution to the EFG have different signs. It thus seems safe to conclude that the iron atoms in FeCoP populate the MeII position. A similar analysis of the Mössbauer spectra for CrFeP and MnFeP as reported by Fruchart et al. (*22*) indicates that in these compounds iron occupies the MeI site.

In an earlier paper (*2*), the ordering of the metal atoms in ternary anti-$PbCl_2$-type compounds was discussed from the size-factor point of view. Following the principle of good space filling, the larger metal atoms should preferentially occupy the MeII positions, which have the highest coordination number, while the smaller metal atoms should occupy the MeI positions. If the Goldschmidt metal atom radii are used for size comparisons it turns out that only the cobalt atoms are smaller than the iron atoms in the ternary phosphides investigated. Accordingly, the iron atoms should occupy the MeI sites in all compounds except FeCoP. The experimental evidence already presented actually agrees with this simple size-factor rule. It seems somewhat surprising, however, that the size-factor effect alone should be sufficient to produce ordering particularly in the case of FeCoP, where the difference in radii between the two metal atom species is only a few hundredths of an angstrom. Undoubtedly, the electronic states of the component atoms are fundamentally important factors. It is interesting to observe that the ordering of the transition metal atoms can be correlated with the number of *d* electrons of the various metal atom species: the atoms with the highest number of *d* electrons

populate the MeI-type positions preferentially. In the case of FeRuP, where the two kinds of metal atom have the same number of *d* electrons, the size-factor rule has to be invoked in order to explain the ordering observed. A hypothetical FeRhP phase would provide a crucial test material, since the "*d*-electron rule" predicts preferential population of iron on the MeII sites while the "size-factor rule" predicts ordering of the iron atoms on the MeI positions. Unfortunately, attempts in the present work to synthesize an FeRhP phase with the anti-$PbCl_2$ structure were unsuccessful.

While the interpretation of the Mössbauer spectra, together with the assignment of the iron atoms to the two possible types of crystallographic position, appears to be reasonably well established for the anti-$PbCl_2$-type phosphides, the situation is less clear for the hexagonal Fe_2P phase.

The difference in Debye temperatures, discussed in Subsections 5.3 and 5.4, can act as a guide in assigning the observed sets of lines to crystallographic positions. The structure of Fe_2P has not been accurately refined using single crystals; however, the single-crystal structure refinements of the two compounds Mn_2P and Ni_2P (*27*) indicate a significant difference between the individual isotropic temperature factors for the two metal atom positions MeI and MeII, the Debye parameter *B* being 0.2–0.4 Å^2 larger for the MeII positions. The phosphides Mn_2P and Ni_2P are both isostructural with Fe_2P, and by analogy it may be inferred that MeII in Fe_2P is associated with a larger Debye parameter *B*, and hence a smaller recoil free fraction. From the definition of the Debye temperature factor *B* in X-ray diffraction,

$$B = 8\pi^2\langle x^2\rangle,$$

and the expression for the recoil-free fraction

$$f = \exp -\frac{4\pi^2\langle x^2\rangle}{\lambda^2},$$

where $\langle x^2\rangle$ is the mean square amplitude of the lattice vibrations, the ratio of recoil-free fractions for the two sites can be expressed in terms of the difference in temperature factors as:

$$f_{II}/f_I = \exp -\frac{1}{2\lambda^2}(B_{II} - B_I).$$

A difference at room temperature of

$$0.2 \leqslant B_{II} - B_I \leqslant 0.4,$$

as found for Mn_2P and Ni_2P, corresponds to an intensity ratio in the Mössbauer spectrum of

$$0.76 \leqslant f_{II}/f_I \leqslant 0.87,$$

when λ is taken as 0.87 Å. This corresponds to the wavelength of the 14.4-keV γ-line used in Mössbauer measurements on ^{57}Fe. From the observed intensity differences for Fe_2P and FeNiP, which are very close to the estimated values, it is then possible to assign the d^5 configuration [isomer shift equal to 0.18 mm/sec (Fe_2P) and 0.19 mm/sec (FeNiP)] to the MeII position. This is then quite opposite to the assignment one would make in analogy to the $Co_{2-x}Fe_xP$ results. In Fe_2P, the MeI type iron has four phosphorus neighbours in a slightly distorted tetrahedral arrangement, whereas around the MeII positions, five phosphorus neighbours are situated at the corners of a square-based pyramid. At first sight it would appear that the lattice contribution to the EFG should be smaller at the MeI positions. It is evidently the different phosphorus environments that has led other investigators (*7*, *18*, *21*, *22*) to their assignment of crystallographic positions. The nearest neighbours have, of course, the largest influence on the central ion, but one should also take the effect from a wider range of surrounding ions into consideration. Assuming that the ions in the lattice can be described as point charges we have, therefore, calculated the lattice contribution to the EFG for Fe_2P and Co_2P using a computer. It turns out that for Fe_2P the contribution is *equally* large for both the crystallographic positions. For Co_2P the contribution is *twice as large* for the MeI position as for the MeII position. The reason why we still obtain a larger quadrupole splitting for the MeII position in the $Co_{2-x}Fe_xP$ compounds is due to the difference in electron configuration. In view of the above we therefore make the tentative assignment of experimental results to crystallographic positions as is shown in Table IV. This assignment will be tested by neutron diffraction measurements on Fe_2P, since the observed difference in hyperfine field indicates a corresponding difference in atomic moment. Such measurements are under way.

Concerning Fe_3P, it is not possible at present to extract any detailed information. This compound has a complicated magnetic structure, but it is hoped that the neutron diffraction work will further clarify the situation.

7. Conclusions

The present investigation has given relatively accurate values for several parameters of importance in the study of chemical bonding and magnetism. It is, however, not yet possible to draw any far-reaching conclusions. Instead, the information pre-

sented should mainly serve as the basis for further investigations using both the Mössbauer effect and other experimental techniques. The investigation has shown that the three binary iron phosphides FeP, Fe_2P, and Fe_3P are quite complicated compounds with regard to their magnetic behaviour. The studies of the ternary phosphides have shown that the Mössbauer technique is a very useful tool for determining the manner in which crystallographic ordering takes place. Even if the ordering of the transition metal atoms seems to follow a simple pattern, much further knowledge about the fundamental electronic interactions is required before the observed phenomena can be satisfactorily explained.

Acknowledgments

Financial support from the Swedish Natural Science Research Council is gratefully acknowledged.

References

1. S. RUNDQVIST, *Ark. Kemi* **20**, 67 (1962).
2. S. RUNDQVIST AND P. NAWAPONG, *Acta Chem. Scand.* **20**, 2250 (1966).
3. R. WÄPPLING, E. KARLSSON, AND S. RUNDQVIST, UUIP-488 (1966).
4. S. RUNDQVIST, *Acta Chem Scand.* **14**, 1961 (1960).
5. S. RUNDQVIST, *Acta Chem. Scand.* **16**, 1 (1962).
6. R. WÄPPLING, *Ark. Fys.* **33**, 337 (1967).
7. A. GÉRARD, *Bull. Soc. Belge Phys.* **1**, 43 (1966).
8. K. SCHUBERT, "Kristallstrukturen zweikomponentiger Phasen," Springer-Verlag, Berlin/Göttingen/Heidelberg, 1964.
9. P. IMBERT, A. GÉRARD, AND M. WINTENBERGER, C.R. *Acad. Sci.* **256**, 4391 (1963).
10. A. A. TEMPERLEY AND H. W. LEFEVRE, *J. Phys. Chem Solids* **27**, 85 (1966).
11. J. DANON, *Tech. Rep. Ser., Int. At. Energy Ag.* **50**, 8 (1966).
12. SHU SHIBA, *J. Phys. Soc. Jap.* **15**, 581 (1960).
13. M-C. CADEVILLE, Thesis, University of Strasbourg, 1965
14. B. F. STEIN AND R. H. WALMSLEY, *Phys. Rev.* **148**, 93 (1966).
15. A. ROGER AND R. FRUCHART, *C.R.H. Acad. Sci.* **264**, 50 (1967).
16. J. BONNEROT, R. FRUCHART, AND A. ROGER, *Phys. Lett A26*, 536 (1968).
17. D. BELLAVANCE, M. VLASSE, B. MORRIS, AND A. WOLD *J. Solid State Chem.* **1**, 82 (1969).
18. R. E. BAILEY AND J. F. DUNCAN, *Inorg. Chem.* **6**, 144 (1967).
19. J. P. SÉNATEUR, A. ROGER, R. FRUCHART, AND J CHAPPERT, *C.R. Acad. Sci. Ser. C* **269**, 1385 (1969).
20. R. H. BEAUMONT, H. CHIHARA, AND J. A. MORRISON *Phil. Mag.* **5**, 188 (1960).
21. K. SATO, K. ADACHI, AND E. ANDO, *J. Phys. Soc. Jap* **26**, 855 (1969).
22. R. FRUCHART, A. ROGER, AND J. P. SÉNATEUR, *J. Appl Phys.* **40**, 1250 (1969).
23. W. KÜNDIG, *Nucl. Instr. Methods* **48**, 219 (1967).
24. T. C. GIBB AND N. N. GREENWOOD, *IAEA Techn. Repor Series* **50**, 143 (1966).
25. E. FRUCHART, A.-M. TRIQUET, AND M. R. FRUCHART *Ann. Chim. (Paris)* **9**, 323 (1964).
26. C. WILKINSON, personal communication.
27. R. INGALLS, *Phys. Rev. A133*, 787 (1964).
28. E. DAHL, *Acta Chem. Scand.* **23**; 2677 (1969).
29. S. RUNDQVIST AND P. NAWAPONG, *Acta Chem. Scand* **19**, 1006 (1965).
30. S. RUNDQVIST AND F. JELLINEK, *Acta Chem. Scand.* **13** 425 (1959).
31. D. AGRESTI, M. BENT, AND B. PERSSON, *Nucl. Instr Methods* **72**, 235 (1969).